Jie Hou

Education

Rice University 09/2012—Present
Ph.D. Candidate in Geophysics, Earth Science

China University of Petroleum(East China) 09/2008—06/2012
B.S. in Exploration Geophysics
Thesis: *High Order Finite-difference Modeling of Acoustic and Elastic Wave*

Research Interest

- True Amplitude Seismic Imaging and Inversion
- Acceleration of Least Squares Migration
- Inversion Velocity Analysis

An Approximate Inverse to the Extended Born Modeling Operator

Jie Hou

TRIP 2014 Review Meeting

May 1st, 2015

Slides based on same title paper submitted to Geophysics

Linearized Inverse Problem

TRIP

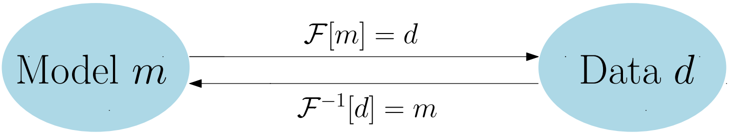

Born Approximation = Linearized Seismic Inverse Problem

- Model Separation

$$m = m_0 + \delta m$$

- First Order Approximation

$$\mathcal{F}[m] \approx \mathcal{F}[m_0] + F[m_0]\delta m$$

- Linearized Map

$$F[m_0]\delta m \to \delta d$$

Given $m_0(\mathbf{x})$, $\delta d(\mathbf{x_r}, t; \mathbf{x_s})$, find $\delta m(\mathbf{x})$ to fit the data:

$$\boxed{F[m_0]\delta m \simeq \delta d}$$

Imaging	**Inversion**
▸ Locate the reflector	▸ Recover the reflector
▸ Kinematically	▸ Kinematically & Dynamically
▸ Adjoint Operator F^*	▸ Inverse Operator F^{-1}
▸ RTM	▸ True Amplitude RTM

Born Modeling and Migration Operator

$$F[v]\delta v(\mathbf{x_r}, t; \mathbf{x_s}) = \frac{\partial^2}{\partial t^2} \int d\mathbf{x} \int d\tau \frac{2\delta v(\mathbf{x})}{v^3(\mathbf{x})} G(\mathbf{x}, \mathbf{t} - \tau; \mathbf{x_r}) G(\mathbf{x}, \tau; \mathbf{x_s})$$

$$F^*[v]d(\mathbf{x}) = \frac{2}{v^3(\mathbf{x})} \int d\mathbf{x_s} d\mathbf{x_r} dt d\tau \, G(\mathbf{x}, \tau; \mathbf{x_s}) \frac{\partial^2 d(\mathbf{x_r}, t; \mathbf{x_s})}{\partial t^2} G(\mathbf{x}, t - \tau; \mathbf{x_r})$$

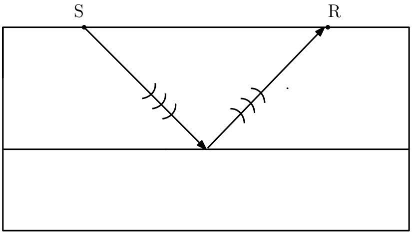

(a) Born Modeling

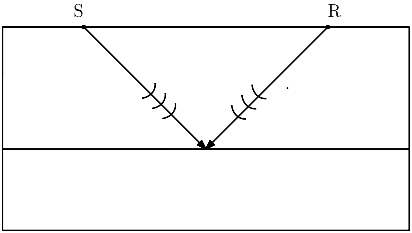

(b) Born Migration

Extended Model

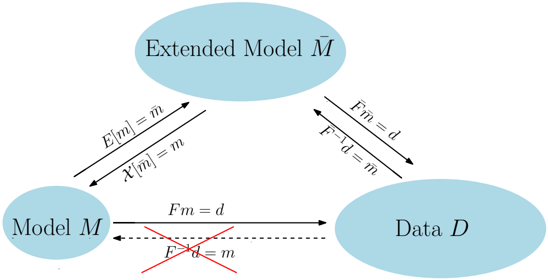

$\mathcal{M}$ = physical model space $\bar{\mathcal{M}}$ = bigger extended model space

$\bar{F} : \bar{\mathcal{M}} \to \mathcal{D}$ extended modeling operator

Extension Property: $E[\mathcal{M}] \subset \bar{\mathcal{M}}$; $m \in \mathcal{M} \to \bar{F}m = Fm$

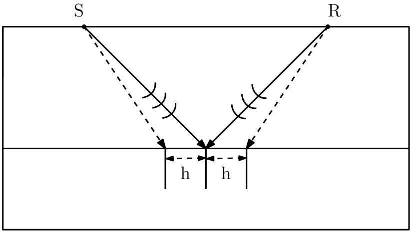

Subsurface Extension : $2\mathbf{h}$ = Difference between subsurface scattering points (subsurface offset)

Physical meaning : action at a positive distance

Extend the operator by permitting δv to also depend on (half) offset $\mathbf{h}$.

Extended Born Modeling and Migration Operator

$$\bar{F}[v]\delta v(\mathbf{x_s}, \mathbf{x_r}, t) = \frac{\partial^2}{\partial t^2} \int d\mathbf{x} d\mathbf{h} d\tau \, G(\mathbf{x}+\mathbf{h}, t-\tau; \mathbf{x_r}) \frac{2\delta v(\mathbf{x}, \mathbf{h})}{v^3(\mathbf{x})} G(\mathbf{x}-\mathbf{h}, \tau; \mathbf{x_s})$$

$$\bar{F}^* d(\mathbf{x}, h) = \frac{2}{v^3(\mathbf{x})} \int d\mathbf{x_s} d\mathbf{x_r} dt d\tau \, G(\mathbf{x}-\mathbf{h}, \tau; \mathbf{x_s}) G(\mathbf{x}+\mathbf{h}, t-\tau; \mathbf{x_r}) \frac{\partial^2 d(\mathbf{x_r}, t; \mathbf{x_s})}{\partial t^2}$$

Extended Kirchhoff Operator

Fons ten Kroode (2012) constructed the inverse of the extended Kirchhoff Operator (in asymptotic sense) :

Fons ten Kroode,2012

$$\tilde{K}i = \frac{1}{2\pi}\int d\mathbf{x}d\mathbf{h}d\omega e^{-i\omega t}G(\mathbf{x_r},\mathbf{x}+\mathbf{h},\omega)\frac{\partial i(\mathbf{x},\mathbf{h})}{\partial z}G(\mathbf{x}-\mathbf{h},\mathbf{x_s},\omega)$$

$$\tilde{I}d = \frac{32}{\pi v^2(\mathbf{x})}\int d\mathbf{x_r}d\mathbf{x_s}d\omega(-i\omega)\frac{\partial G^*(\mathbf{x}+\mathbf{h},\mathbf{x_r},\omega)}{\partial z_r}d(\mathbf{x_r},\mathbf{x_s},\omega)\frac{\partial G^*(\mathbf{x_s},\mathbf{x}-\mathbf{h},\omega)}{\partial z_s}$$

(http://iopscience.iop.org/0266-5611/28/11/115013)

Can we construct a similar operator to extended Born Modeling Operator?

Construction of the Inverse Operator

Asymptotic Analysis of the Normal Operator $\bar{F}[v]^* \bar{F}[v]\delta v(\mathbf{x}, h)$

Extended Born Modeling Operator and its Adjoint

$$\bar{F}[v]\delta v = \frac{\partial^2}{\partial t^2} \int d\mathbf{x} d\mathbf{h} d\tau \, G(\mathbf{x}+\mathbf{h}, t-\tau; \mathbf{x_r}) \frac{2\delta v(\mathbf{x}, \mathbf{h})}{v^3(\mathbf{x})} G(\mathbf{x}-\mathbf{h}, \tau; \mathbf{x_s})$$

$$\bar{F}^*[v]d = \frac{2}{v^3(\mathbf{x})} \int d\mathbf{x_s} d\mathbf{x_r} dt d\tau \, G(\mathbf{x}-\mathbf{h}, \tau; \mathbf{x_s}) G(\mathbf{x}+\mathbf{h}, t-\tau; \mathbf{x_r}) \frac{\partial^2 d(\mathbf{x_r}, t; \mathbf{x_s})}{\partial t^2}$$

- Step 1 High Frequency Approximation
- Step 2 Principle of Stationary Phase
- Step 3 Modify adjoint operator by some Scaling and Filters

Where miracle happens

- Key element left $\frac{a_s^2 a_r^2}{\sqrt{|det\ Hess|}}$
- Relation between amplitudes and Beylkin determinant

(Bleistein, N.; Zhang, Y.; Xu, S.; Zhang, G.; Gray, S, 2005)

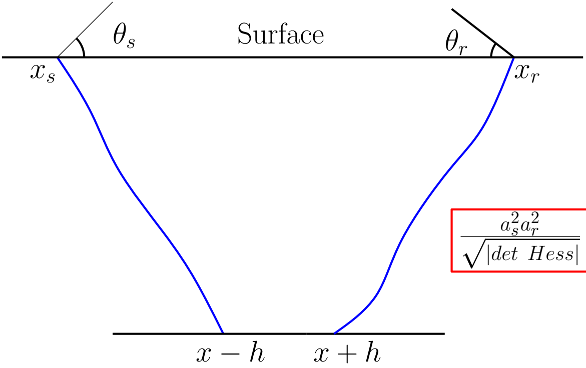

$$\boxed{\frac{a_s^2 a_r^2}{\sqrt{|det\ Hess|}} \sim \frac{cos\theta_s}{v_s}\frac{cos\theta_r}{v_r}}$$

An Approximate Inverse

$$\bar{F}[v_0]^\dagger = W_{\rm model}^{-1}[v_0]\bar{F}[v_0]^* W_{\rm data}[v_0].$$

- $W_{\rm model}^{-1} = 4v_0^5 LP,\ W_{\rm data} = I_t^4 D_{z_s} D_{z_r}$
- $L = \sqrt{-\nabla^2_{(x,z)}}\sqrt{-\nabla^2_{(h,z)}}$
- P is *integral* operator with computable kernel ($P \approx 1$ near $h = 0$ or if horizontal velocity variation is small)
- I_t is the time integral
- D_{z_s}, D_{z_r} are the source and receiver depth derivative.

- 2-8 Finite Difference
- 2.5-5-30-35 Hz Bandpass Wavelet
- $dx = dz = dz = 10m, dt = 1ms$
- Dense sampled sources (every 40m)
- Fixed Spread Receivers
- Absorbing Boundary, except free surface on the top

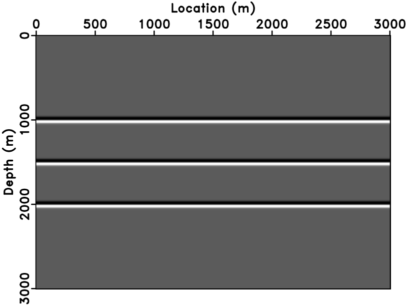

Reflectivity Model

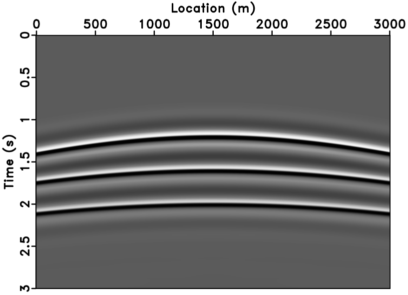

One-shot Born Data

Extended Migration Result

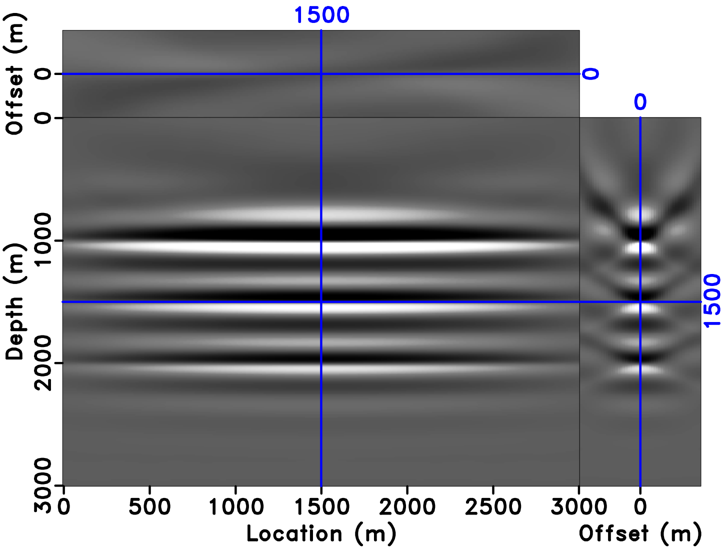

Extended Inversion Result

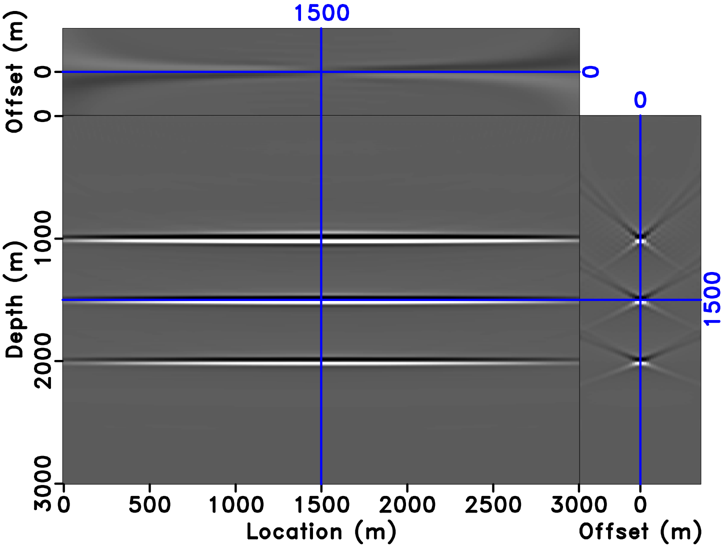

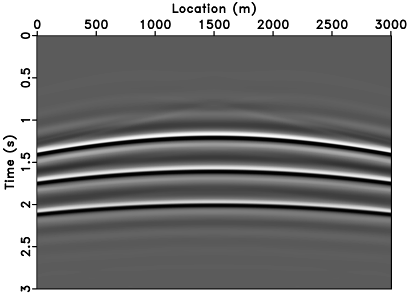

Resimulated Data

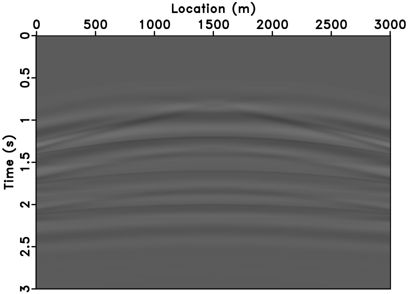

Data Residual
(= *13.6% ||observed data||*)

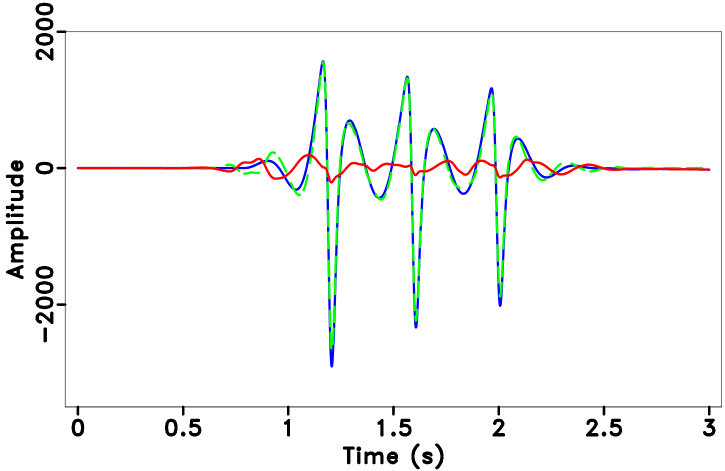

Figure: One trace (middle) comparison between the original data(blue) and resimulated data(green). The difference is shown as the red line.

From extended to nonextended model

TRIP

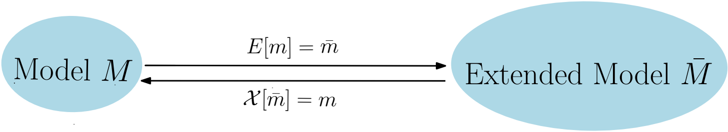

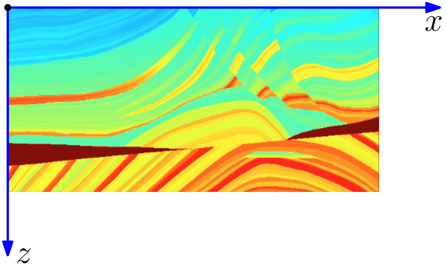

$E[\delta v]$:

$$\delta v(\mathbf{x}, h) = \delta v(\mathbf{x})\delta(h)$$

$\mathcal{X}[\bar{\delta v}]$:

$$\delta v(\mathbf{x}) = \int \delta v(\mathbf{x}, h)\Phi(h)\mathrm{d}h$$

where $\Phi(0) = 1$

From extended to nonextended model

TRIP

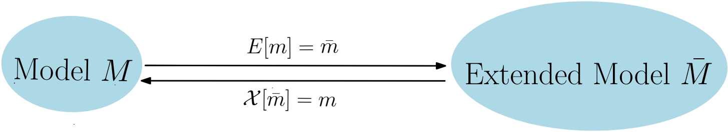

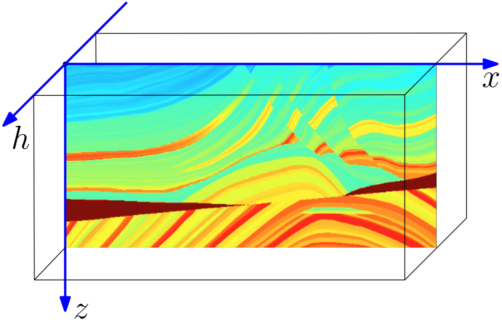

$E[\delta v]$:

$$\delta v(\mathbf{x}, h) = \delta v(\mathbf{x})\delta(h)$$

$\mathcal{X}[\bar{\delta v}]$:

$$\delta v(\mathbf{x}) = \int \delta v(\mathbf{x}, h)\Phi(h)\mathrm{d}h$$

where $\Phi(0) = 1$

Non-extended Inversion Result

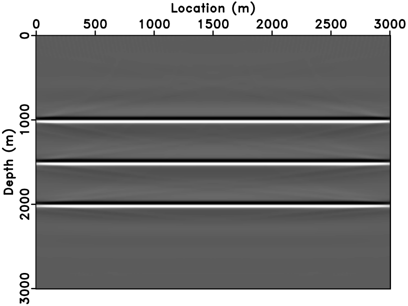

Non-extended Inversion Result

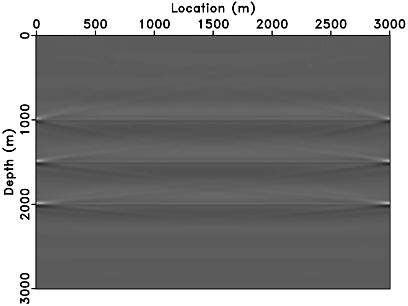

Model Residual
(= *19.1%* $||model||$)

$$\delta v(\mathbf{x}) = \sum_h \delta v(\mathbf{x}, h)$$

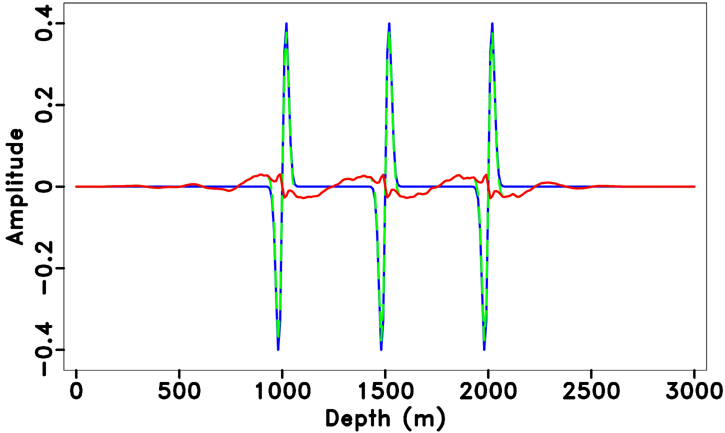

Figure: One trace (middle) comparison between the reflectivity model (blue) and non-extended inversion result (green). The difference is shown as the red line.

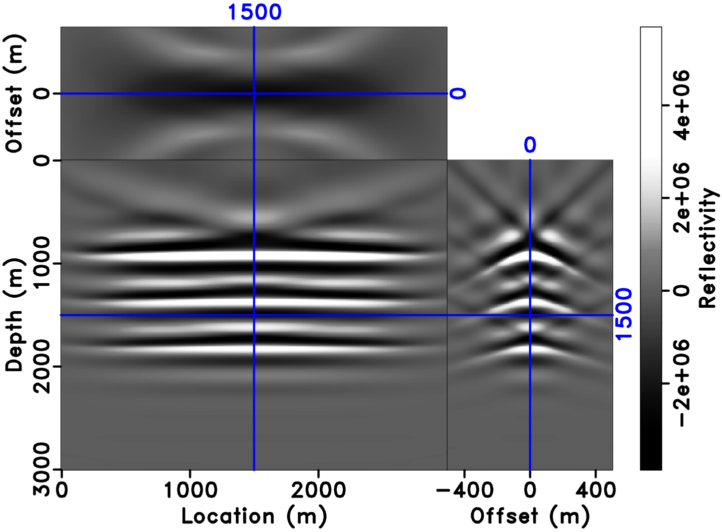
1500
0
0
1500
Offset (m)
Depth (m)
0
0
1000
2000
3000
0
1000
2000
Location (m)
-400
0
400
Offset (m)
4e+06
2e+06
0
-2e+06
Reflectivity

Extended Inversion Result-Wrong Background

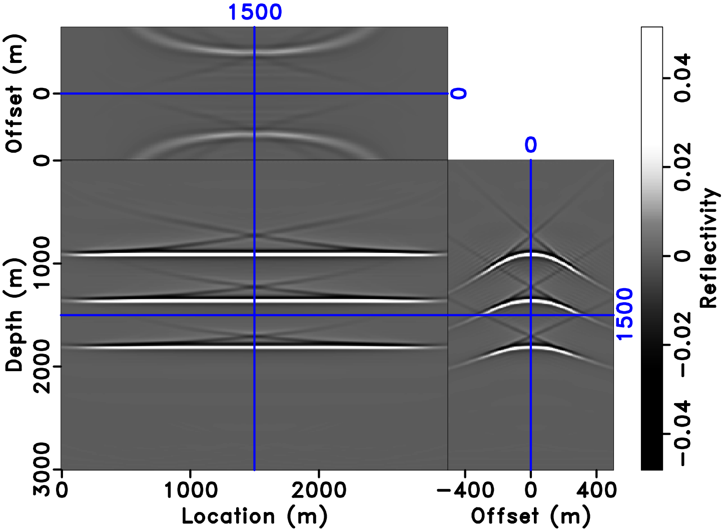

Resimulated Data-Wrong Background

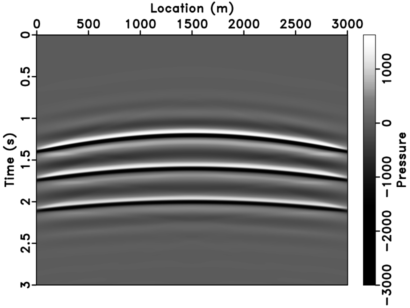

Resimulated Data

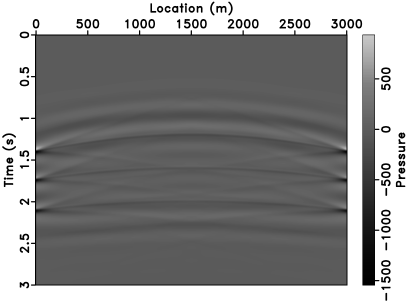

Data Residual

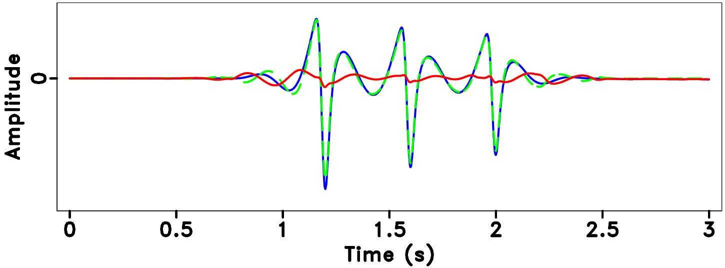

Figure: One trace (middle) comparison between the original data(blue) and resimulated data(green). The difference is shown as the red line.

Stacked Image-Wrong Background

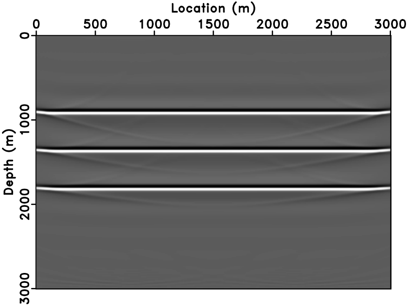

Stacked Image

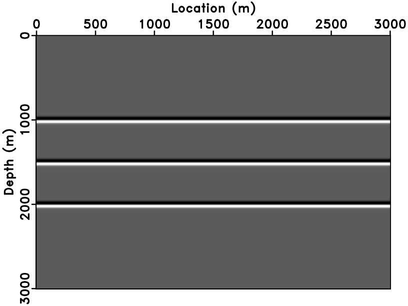

Reflectivity Model

Apply $D_{z_s} D_{z_r}$-Naive Implementation

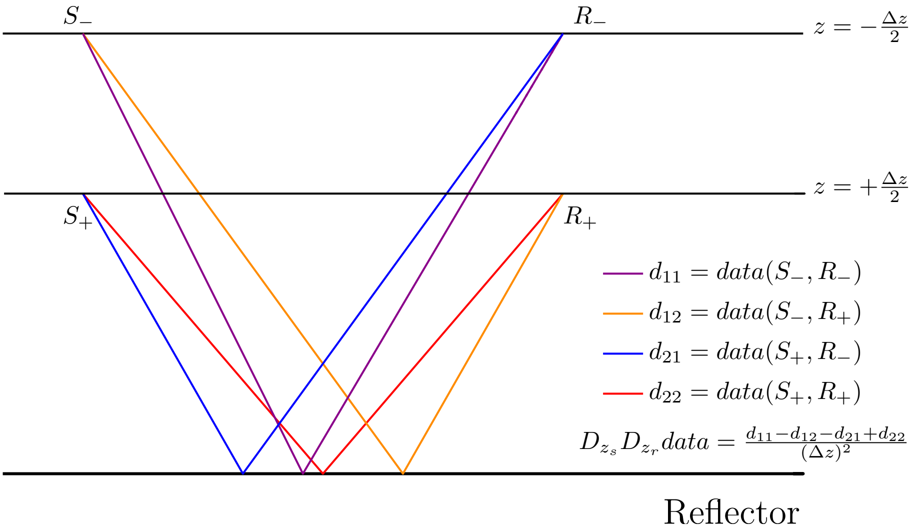

Apply $D_{z_s} D_{z_r}$-Free Surface Simulation

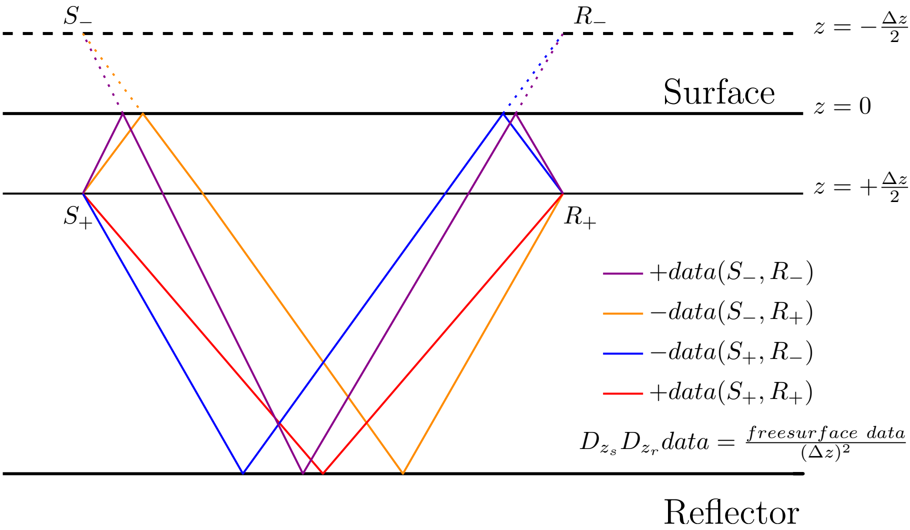

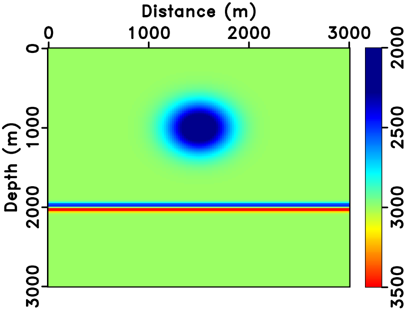

Velocity Model

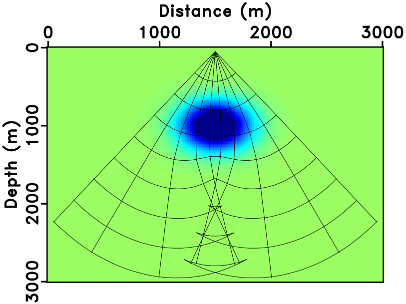

Wavefronts and Rays

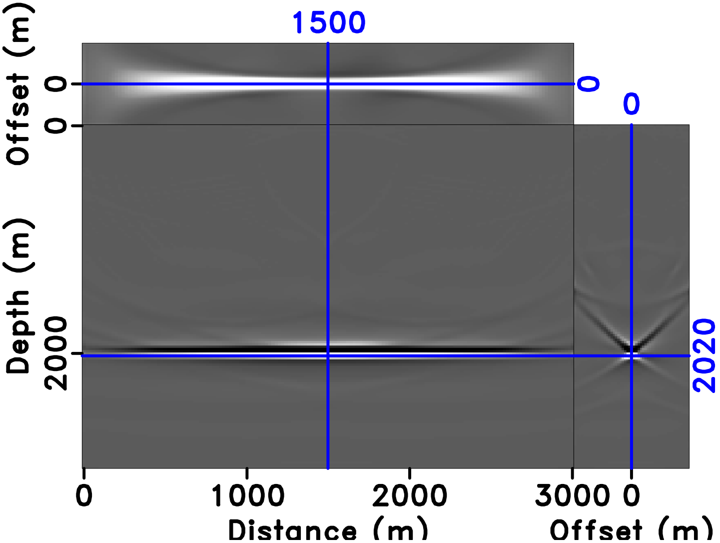
1500
0
0
2020
Offset (m)
0
0
Depth (m)
2000
0
1000
2000
3000 0
Distance (m)
Offset (m)

Resimulated Data

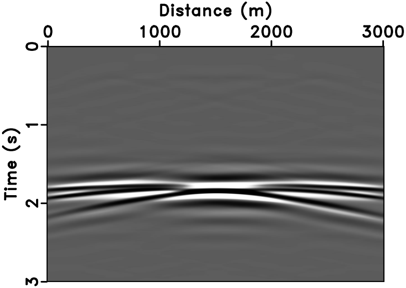

Resimulated Data

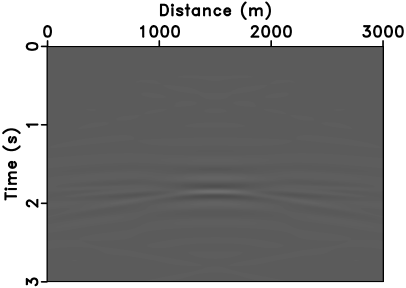

Data Difference
$=10.4\% ||\textit{observed data}||$

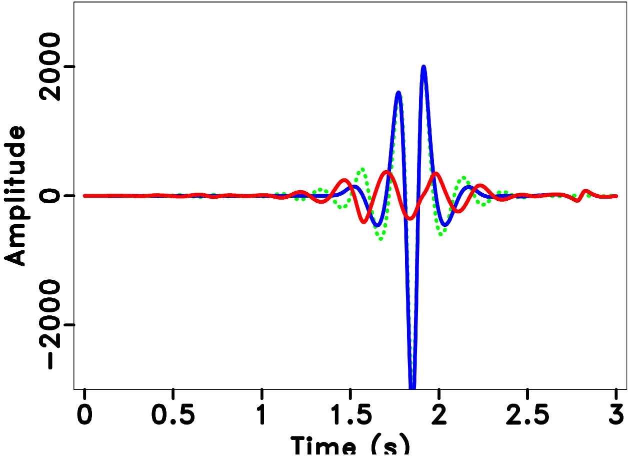

Figure: One trace (middle) comparison between the original data(blue) and resimulated data(green). The difference is shown as the red line.

Non-extended Inversion

TRIP

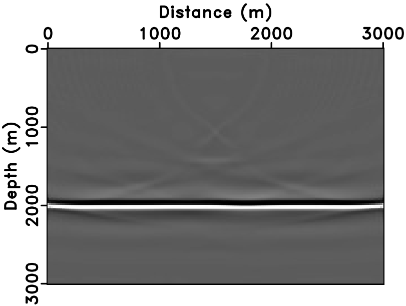

Non-extended Inversion Result

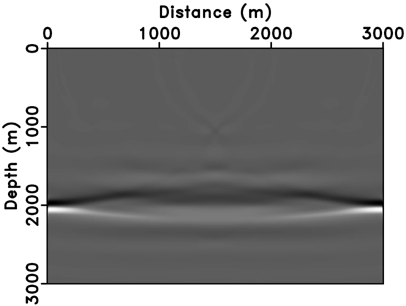

Model Difference

$=21.3\% \ ||model||$

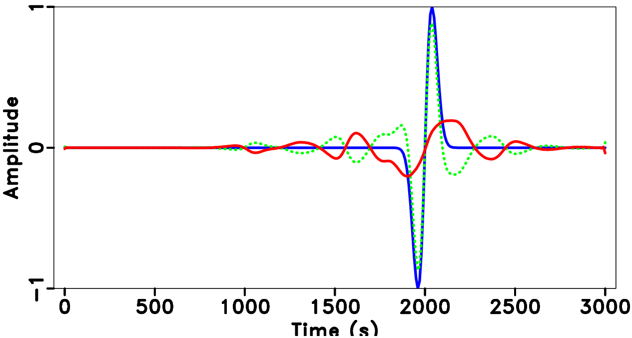

Figure: One trace (middle) comparison between the reflectivity model (blue) and non-extended inversion result (green). The difference is shown as the red line.

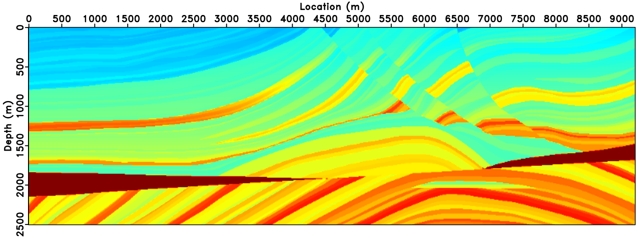

Marmousi Model

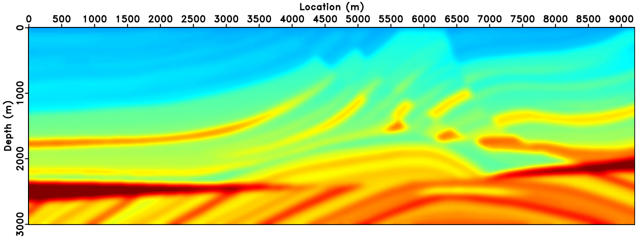

Background Velocity Model

Extended Inversion Result

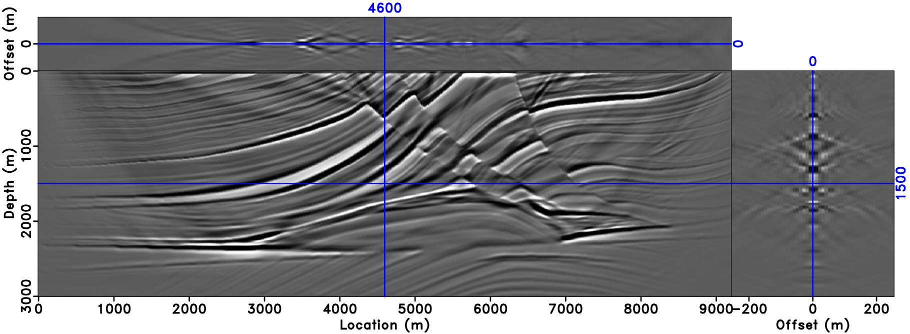

Resimulation Comparison

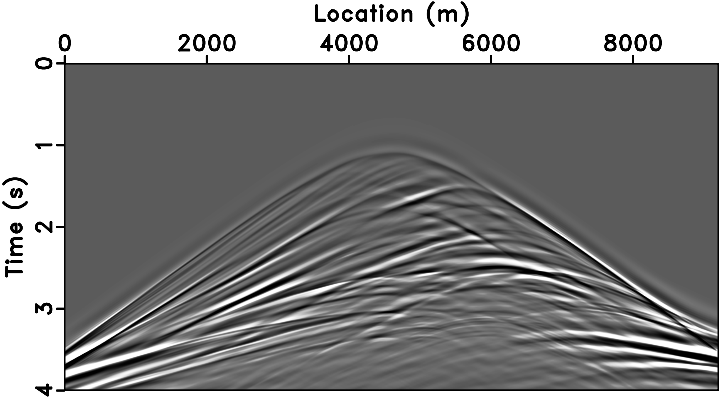

Original Data

Resimulation Comparison

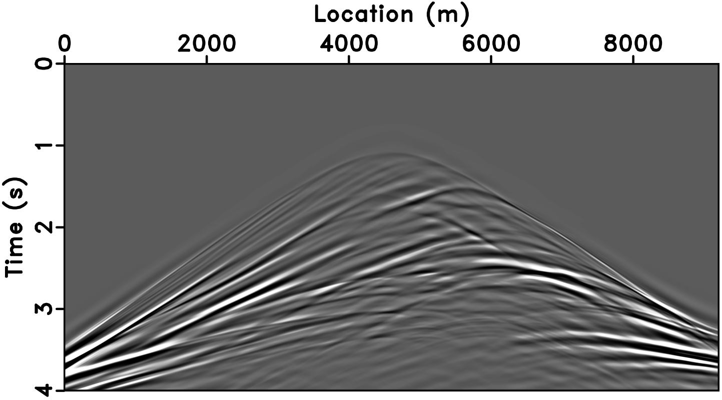

Resimulated Data

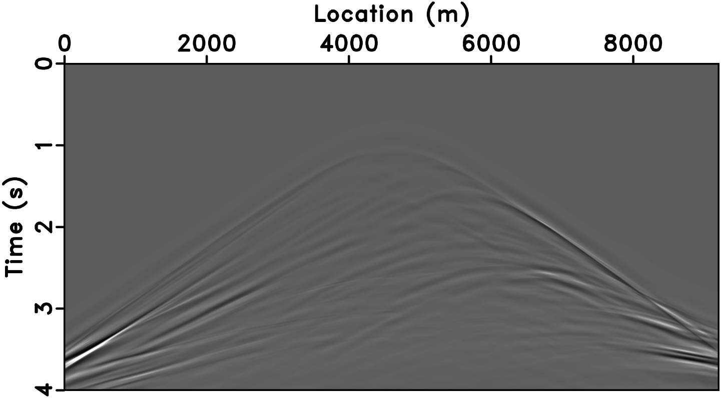

Data Difference

One Trace comparison

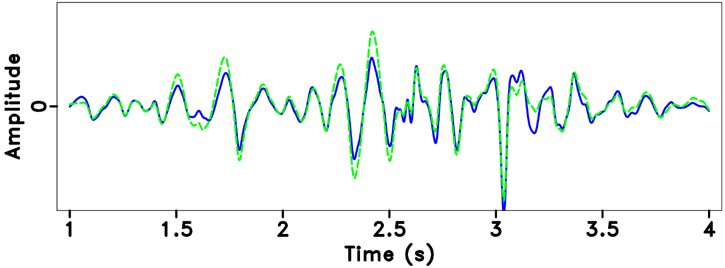

Figure: One trace (middle) comparison between the original data(blue) and resimulated data(green)

Marmousi Model

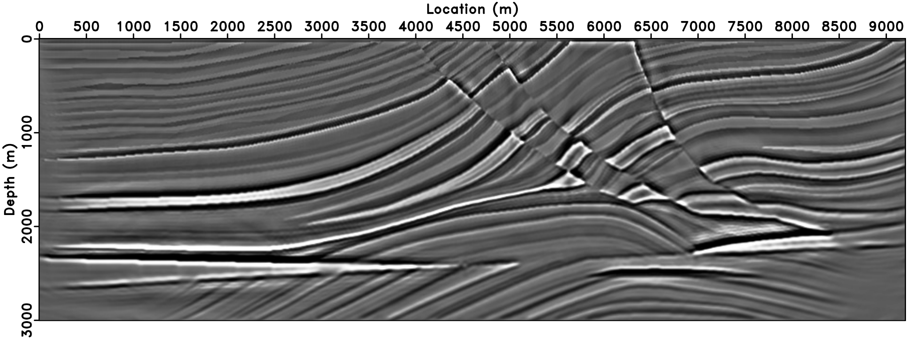

Nonextended Inversion Result

Marmousi Model

TRIP

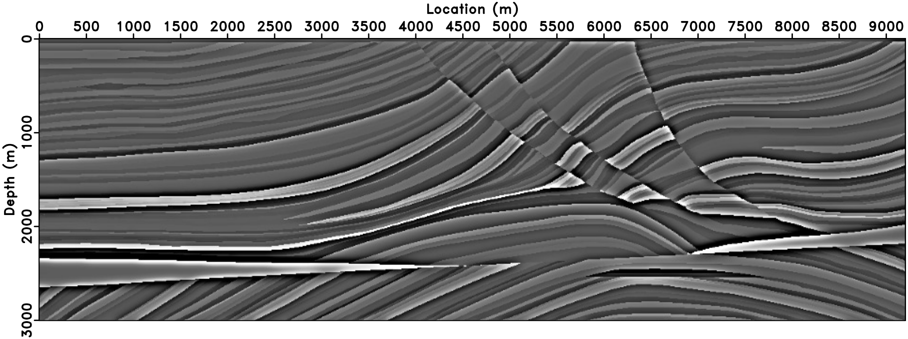

Reflectivity Model

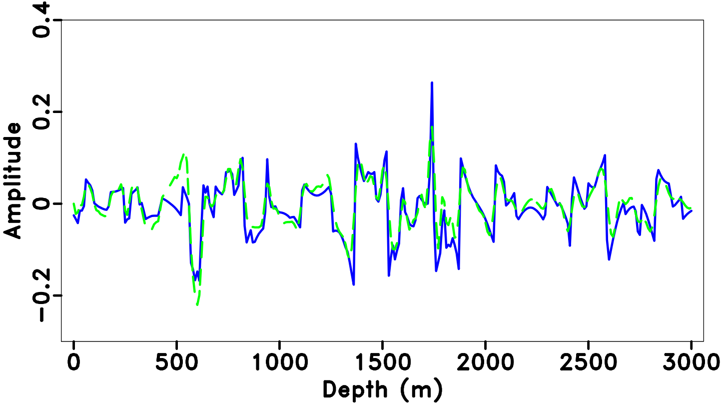

Figure: One trace (middle) comparison between the original data(blue) and resimulated data(green))

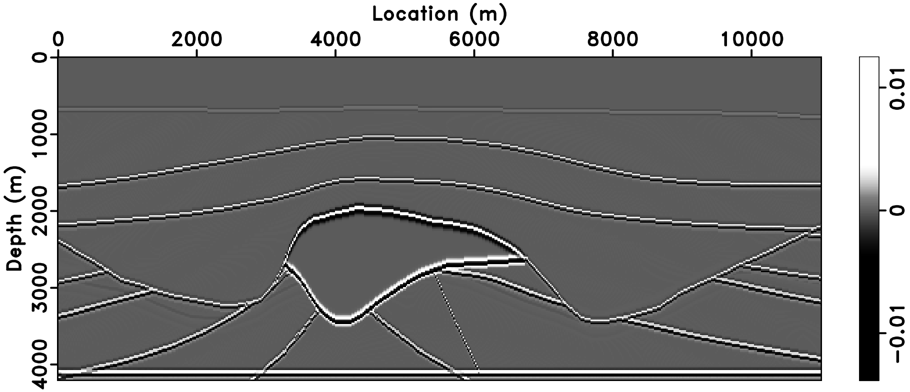

Reflectivity Model

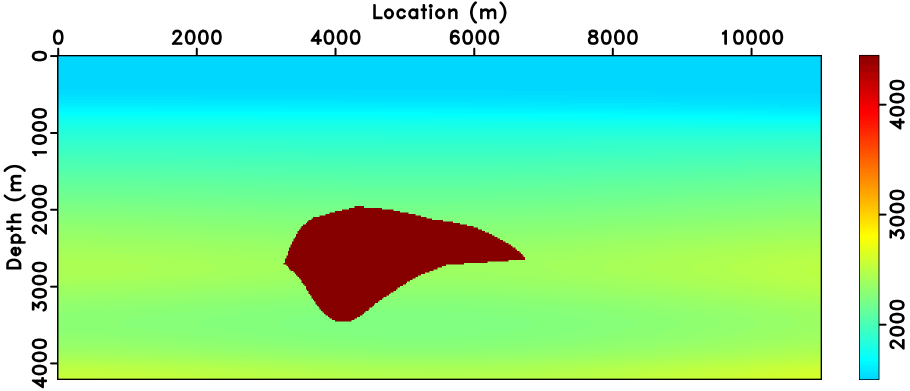

Background Model

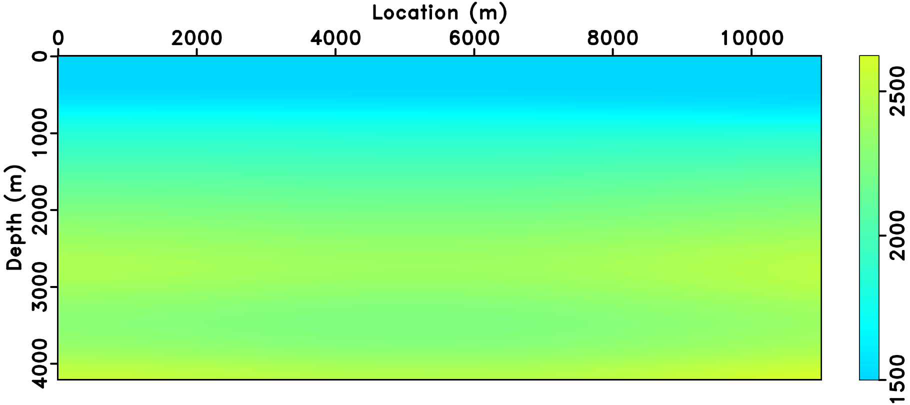

Background Model (Salt Removed)

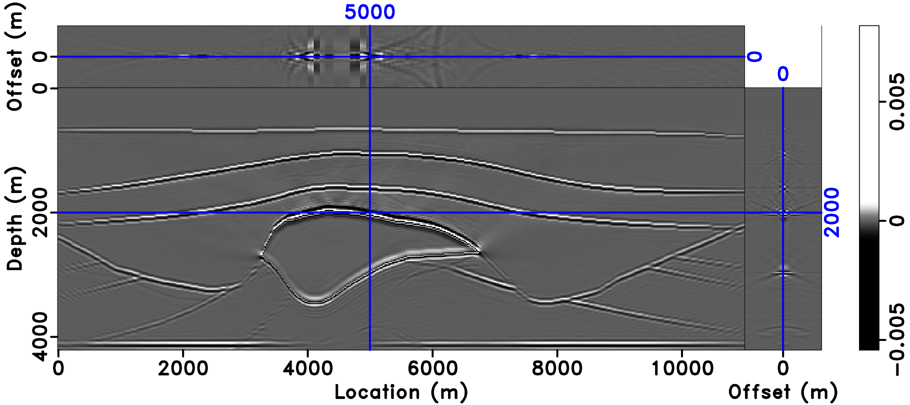

Extended Inversion Result

SEG/EAGE Salt Model-Salt Removed

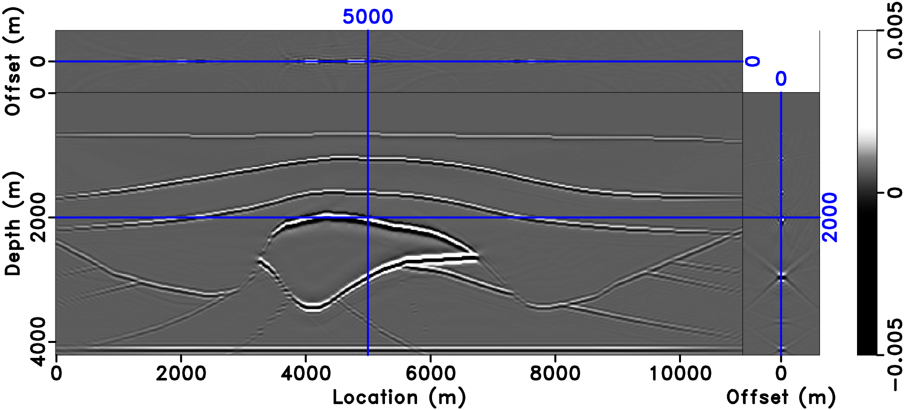

Extended Inversion Result

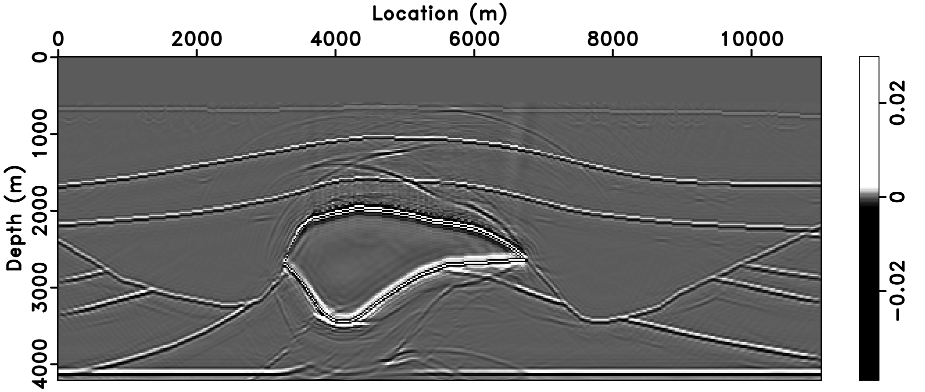

Nonextended Inversion Result

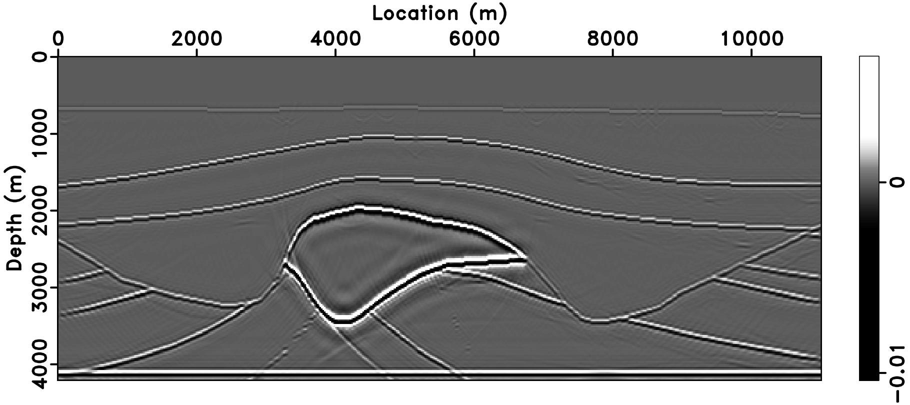

Nonextended Inversion Result

Takeaway Messages

- Subsurface offset extended RTM can be modified into an asymptotic inverse to the extended Born Modeling Operator
- Although the derivation is based on asymptotic theory, the implementation doesn't involve any ray computation
- The new inverse operator can approximate the ELSM result
- The new inverse operator can also produce non-extended inversion, which can approximate LSM

Acknowledgement

- Fons ten Kroode, Jon Sheiman, Henning Kuehl, Peng Shen, Yujin Liu
- TRIP Members and Sponsors
- Shell International Exploration and Production
- Madagascar, SU,TACC, RCSG
- Thank you for listening

SEG/EAGE Salt Model-Difference

TRIP

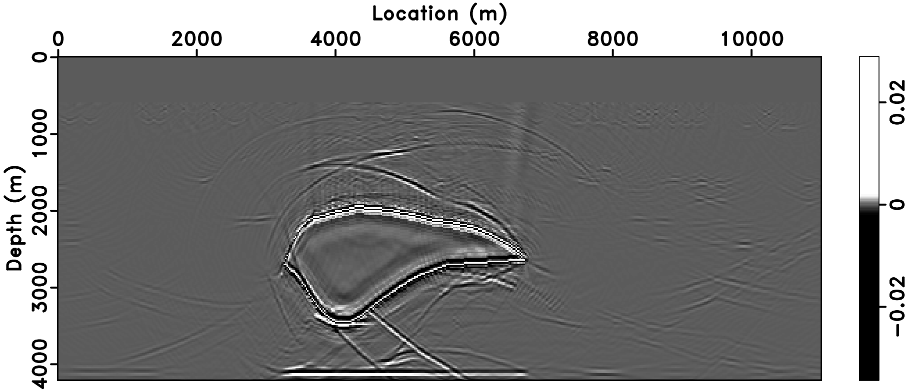

Nonextended Inversion Result Difference